

# Content Based Image Retrieval of Brain MR Images across Different Classes

Abraham Varghese, Kannan Balakrishnan, Reji R. Varghese, and Joseph S. Paul

**Abstract**—Magnetic Resonance Imaging play a vital role in the decision-diagnosis process of brain MR images. For an accurate diagnosis of brain related problems, the experts mostly compares both T1 and T2 weighted images as the information presented in these two images are complementary. In this paper, rotational and translational invariant form of Local binary Pattern (LBP) with additional gray scale information is used to retrieve similar slices of T1 weighted images from T2 weighted images or vice versa. The incorporation of additional gray scale information on LBP can extract more local texture information. The accuracy of retrieval can be improved by extracting moment features of LBP and reweighting the features based on users' feedback. Here retrieval is done in a single subject scenario where similar images of a particular subject at a particular level are retrieved, and multiple subjects scenario where relevant images at a particular level across the subjects are retrieved.

**Keywords**—Local Binary pattern (LBP), Modified Local Binary pattern (MOD-LBP), T1 and T2 weighted images, Moment features.

## I. INTRODUCTION

THE advantage of magnetic resonance imaging over other modalities persuade the radiologists to handle various brain related issues. MRI operates at radio-frequency (RF) range; thus there is no ionizing radiation involved. Furthermore, MRI can generate excellent soft tissue contrast, and has the capability of producing images at any orientation. Moreover the information content present in MR images is extremely rich compared to other imaging modalities as it operates at radio-frequency range.

The first step in reporting of the magnetic resonance images is reviewing of the cross sectional images at various levels. Generally, the inter-patient search which can compare multiple patients and retrieve relevant cases among them will especially help the expert in diagnosis of structure-specific diseases, such as hippocampus or basal ganglia disorders. The retrieval of T1-weighted and T2-weighted images of a same subject at a particular level from a large data base is also quite useful in the decision-diagnosis process as the information available in the images is complementary. The problem of locating desired slices from a large database is challenging due to Inter- and intra patient intensity variations, intensity non-uniformity, misalignment of images due to head motion etc. The intensity values of T1- weighted and T2-weighted mages

of a particular person at a particular level itself vary drastically.

Researchers [1]-[3] considered similar slice retrieval problem on a same class of images by giving importance to similarity of anatomical structures. Unay et al. [4], [5] addressed brain image retrieval problem using Local Binary Patterns (LBP) in which similarity attributes of anatomical structures are extracted using fiducial points which are obtained using a Kanade-Lucas-Tomasi (KLT) transform. In this paper, in order to handle intensity related problems, a local measure called Modified Local Binary Pattern (MOD-LBP) is used which is relevant as MR image is locally smooth. It is obtained by assigning weights to the P-bit binary pattern in LBP, based on the squared difference of individual pixels from the average value. As every pixel in the local neighborhood is involved in the MOD-LBP computation, the method is invariant to some basic geometric transformations and intensity variations locally. In order to achieve reliable image retrieval performance in the presence of global misalignments, the image is converted to polar form ( $r, \theta$ ) by assuming centroid as the origin of the image and thus it avoids registration. Thus features are extracted in such a way that it is invariant to both rotation and translation.

The remainder of this paper is organized as follows. Section II describes the methodology. Section III discusses the experimental results. Finally, discussion and conclusion is presented.

## II. METHODOLOGY

The overview of the image retrieval scheme is shown in Fig. 1. The MOD-LBP image code is computed using a circular neighborhood with P pixels and radius R. The histogram of MOD-LBP are extracted spatially and non-spatially [6]. The MOD-LBP image is converted to polar form ( $r, \theta$ ) in order to compensate for rotation and translation in spatial description of the features by taking centroid as the origin of the image. The output image obtained is of size  $N \times N$  with N points along the r-axis and N points along the  $\theta$ -axis. The pixel value at the non-integer coordinate of the image is estimated using bilinear interpolation. The histogram of MOD-LBP is computed spatially, where the entries of each bin are indexed over angularly partitioned regions. The pixel intensities are brought in the range  $[0, L]$ , where L is a positive integer and normalized histogram of the image is taken as feature vectors for similarity computation. The images in the database are ranked based on the Bhattacharya distance between query and database images. The average

Abraham Varghese is with the Adi Shankara Institute of Engineering and Technology, Kalady, Kerala, India (e-mail: abrahamvarghese77@gmail.com).

Kannan Balakrishnan is with the Cochin University of Science and Technology, Cochin, Kerala, India.

Reji R. Varghese is with the Co-Operative Medical College, Cochin, India.

Joseph S. Paul is with the Indian Institute of Information Technology and Management, TVM, Kerala, India.

rank and accuracy is calculated for a set of query images. A further improvement in the accuracy of retrieval is obtained by

extracting the moment features and reweighting it based on users' feedback.

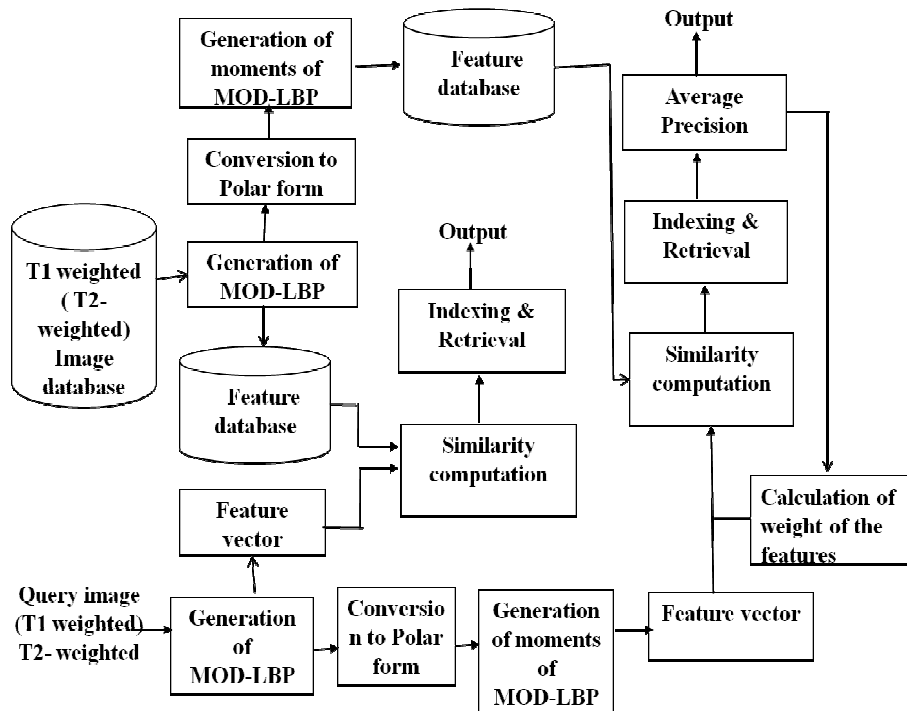


Fig. 1 Block diagram of Image retrieval scheme

#### A. Preprocessing

The image is converted to binary image by applying suitable thresholding. The components (objects) that have fewer than  $P$  (say) pixels are removed from the binary image, resulting only one connected component. The centroid of the binary image is computed using 'REGIONPROPS' operation, which measures a set of properties for each connected component (object) in the binary image. Then resulting image is multiplied with original image for further feature extractions.

#### B. LBP and MOD-LBP

The Local Binary Pattern (LBP) operator is a gray-scale invariant texture primitive, derived from a general definition of texture in a local neighborhood. Due to its discriminative power and computational simplicity, the LBP operator has become a highly popular approach in various computer vision applications, including visual inspection, image retrieval, remote sensing, biomedical image analysis, biometrics, motion analysis, environment modeling, and outdoor scene analysis, etc. LBP is formed by comparing gray value of center pixel ( $g_c$ ) with that of  $P$  neighborhood pixels in the local neighborhood [7], [8].

$$LBP = \sum_{i=0}^{P-1} s(g_i - g_c) 2^i, \quad \begin{cases} s(x) = 1, x \geq 0 \\ 0, x < 0 \end{cases} \quad (1)$$

The operator  $LBP_{P,R}$  is derived based on a symmetric

neighbor set of  $P$  members  $g_i$  ( $i = 0, 1, \dots, P-1$ ) within a circular radius of  $R$ . The signs of the differences (1) in a neighborhood are interpreted as a  $P$ -bit binary number, resulting in  $2^P$  distinct values for the LBP code. One way to eliminate the effect of rotation is to perform a bitwise shift operation on the binary pattern  $P-1$  times and assign the LBP value that is the smallest, which is referred to as rotational invariant LBP,  $LBP^r(P, R)$ .  $LBP^{riu2}(P, R)$  is referred to as rotational invariant LBP with limited number of transitions [7]. The above measures are invariant to monotonic gray level changes because just the sign of the differences only are considered instead of their exact values. In order to account for the changes in contrast and rotational invariance against grayscale shift with respect to the window taken, the definition of the LBP is modified [9] as shown in (2).

$$MOD-LBP(P, R) = \frac{1}{P} \sum_{i=0}^{P-1} s(g_i - g_c)(g_i - \mu)^2 \quad (2)$$

where  $\mu$  is the mean of the  $P$  circular neighborhood pixels and  $R$  is the radius. Bilinear interpolation is applied to the non-integer coordinate points on the image in order to interpolate the pixels. The weights are assigned to the  $P$ -bit binary pattern based on the square of the gray scale difference between neighborhood pixel values and mean gray scale value. The resultant image is formed by assigning the decimal equivalent of the weighted binary number to the central pixel. As MOD-LBP is computed locally, it is invariant to monotonic gray

level change, and it can even resist intra-image illumination variation as long as the absolute gray value differences are not much affected. Normalized histogram of MOD-LBP is taken as feature vector and Bhattacharya distance is used for similarity computation

### C. Feature Description

#### 1. Spatial and Non-Spatial Histogram

In spatial MOD-LBP, the entries of each bin are spatially indexed [6] over angularly partitioned regions as shown in Fig. 2. This will give more meaningful information as the brain slices are quasi-symmetric across the left and right hemispheres. The angular regions are obtained with respect to a reference line which is identified in the preprocessing step. This serves as a translation and rotation invariant reference frame. The histogram of the entire MOD-LBP is taken as features in Non-spatial MOD-LBP.

#### 2. Spatial and Non-Spatial Moments of MOD-LBP

Similar to the method outlined in section 2.C, central moments of even order (12 numbers), Rotational, Scaling, and Translational (RST) invariant features (7 numbers), and eccentricity are extracted from each angularly partitioned regions. The definition of moment features are given in APPENDIX-A. The retrieval performance is evaluated using individual features as well as the features together. Since the presence of the some features degrades the performance of the entire system, we reweight individual features based on its role in the retrieval process [10], [11].

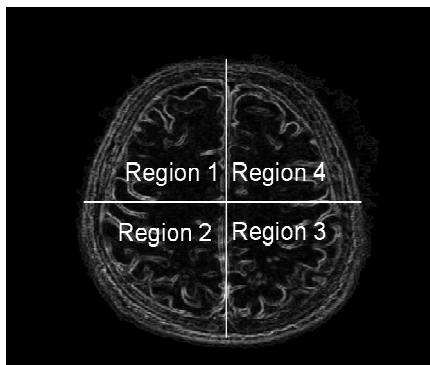


Fig. 2 Four Angularly partitioned regions

### III. RESULTS

The slices (T1&T2 weighted) used in this work are acquired on a 1.5 Tesla, General Electric (GE) – Signa HDxt MR Scanner from Pushpagiri Medical College Hospital, Tiruvalla, Kerala, India. Axial, 2D, 5mm thick slice images, with a slice gap of 1.5mm are acquired with the field-of-view (FOV) of range 220mm to 250mm. The T2 (TR/TE(eff.) of 3500-4500/85-105(eff.) ms) images are collected using Fast Spin Echo (FSE) sequences with a matrix size of 320 X 224 (Frequency X Phase) and a NEX (Averages) of 2. The T1 weighted images (TR/TE of 450-550/8-12ms) were acquired using standard spin echo (SE) sequence with a matrix size of 288 X 192 (Frequency X Phase) and a NEX(Averages) of 2.

We have categorized unregistered Brain MR images of different subjects into 4 levels, for independently evaluating the performance of the histogram based image retrieval method.

- L1. The foramen magnum (The cerebellum with paranasal sinus is present)
- L2. Above the fourth ventricle (Caudate nucleus, thalamus, basal ganglia are seen)
- L3. Mid ventricular section
- L4. Above the ventricle. The Fig. 3 shows the T1 and weighted images of level 3(L3).

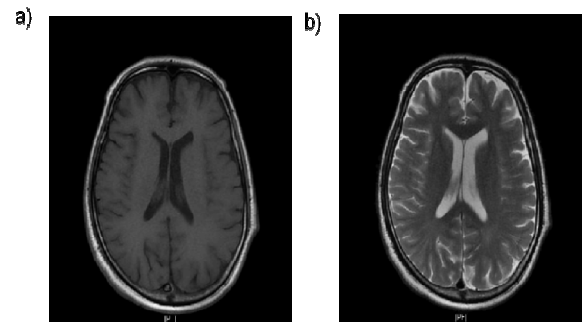


Fig. 3 T1 and T2 weighted images of the level 3 (L3)

In order to test the robustness of MOD-LBP with respect to intensity variations simulated bias fields from the Brain Web MR simulator (20% &40%) are used [12]. These bias fields provide smooth variations of intensity across the image. As the MOD-LBP is calculated locally, intensity inhomogeneity has less sensitivity on it because the bias field in MRI is locally smooth. The degree of dissimilarity between MOD-LBP of original and the degraded images (100 images randomly chosen) are computed using the Bhattacharyya

distance,  $d = 1 - \sum_{i=0}^{L-1} \sqrt{p(i)q(i)}$  where  $p$  and  $q$  are

normalized histograms with L1-bins. The mean dissimilarity scores fall in the range of [0 1], where 0 means that all original images and its degraded images are perfectly similar. Table I shows the effect of bias field in similarity computation between original image and degraded image using Bhattacharyya distance. It is observed that the MOD-LBP computation helps to decrease dissimilarity between original and degraded image. Also as bias field increases the dissimilarity increases and MOD-LBP with window size 3 and 5 shows more or less same dissimilarity.

TABLE I  
THE DISSIMILARITY SCORE BETWEEN ORIGINAL AND DEGRADED IMAGE

Method	Window size	Bias field	
		20%	40%
Histogram		$8.36 \times 10^{-2}$	$12.26 \times 10^{-2}$
MOD-LBP(8,1)	3	$4.93 \times 10^{-2}$	$8.68 \times 10^{-2}$
MOD-LBP(16,2)	5	$4.99 \times 10^{-2}$	$8.83 \times 10^{-2}$

#### A. Retrieval of T2 Weighted Images Similar to T1 Weighted Image across the Subjects

In order to test the performance of the retrieval system we had taken 40 T2 weighted images from L1, 32 images from L2, 32 images from L3 and 40 images from L4 as query image across the subjects and calculated average rank and accuracy of retrieving similar T1 weighted images based on the histogram of different LBP variants. The retrieval performance is evaluated using average rank, which is calculated using the formula,

$$Rank = \frac{1}{N_R} \left( \sum_{i=1}^{N_R} R_i - \frac{N_R(N_R - 1)}{2} \right) \quad (3)$$

$N_R$  represents number of relevant images and  $R_i$  represents the rank at which the  $i^{th}$  relevant image is retrieved [13]. An ideal retrieval algorithm is expected to yield a rank of 1 for all the query images. The Accuracy of the retrieval system for a set of queries is also calculated using the formula,

$$Acc = \left( 1 - \frac{No. of relevant images retrieved}{Total no of relevant images} \right) \quad (4)$$

The experiment is performed by extracting the moment features and reweight the features based on users feedback Table II illustrates the comparison of LBP and MOD-LBP in retrieving first 5 relevant images.

TABLE II  
THE AVERAGE RANK AND ACCURACY IN RETRIEVING FIRST 5 RELEVANT T1-WEIGHTED IMAGES CORRESPONDS TO T2-WEIGHTED IMAGES A) AVERAGE RANK B) ACCURACY

LBP <sup>i</sup> (8,1)				MOD-LBP(8,1)						
LBP <sup>ri</sup> (8,1)		LBP <sup>riu2</sup> (8,1)		Features	Non-spatial		Spatial			
							9angular regions		18angular regions	
a)	b)	a)	b)		a)	b)	a)	b)	a)	b)
				Histogram	9.74	93.6	10	92.9	8.5	94
10.1	93.1	9.9	93.2	Moments	10.6	93.4	5.69	96.1	7.45	94.6
				Rewighted Moments			3.8	97.4	5.6	95.8

The result shows an accuracy of 93.09% in retrieving 5 relevant images using rotational invariant uniform pattern with 8 neighborhood pixels ( $LBP^{riu2}(8,1)$ ). MOD-LBP shows an accuracy of 93.6% using non-spatial histogram features. Spatial LBP histogram using 18 angular regions shows an accuracy of 94%. Results also reveal that replacing histogram with spatial moments improves the accuracy. A further improvement of accuracy is achieved by reweighting the features.

#### B. Single Subject Performance

In order to study the retrieval performance in a single subject scenario, T1- weighted image of a subject similar to its T2-weighted image is retrieved. As our database consists of 20 slices of 20 subjects data, with four landmark slices per subject, there are 20×4 query images. For a query image  $i$ , the images in the database are ranked based on the Bhattacharya distance of the histogram of MOD-LBP between query and database images. The error in the retrieval of images correspond to  $i^{th}$  query image is defined as  $Err(i) = \sum_{j=1}^{k-1} |S_j - S_k|$  where  $S_j$  is the slice number at rank  $j$ , and  $k$  is the rank of the relevant slice. In order to reduce the error, moment features central moments of even order (12 numbers), Rotational, Scaling, and Translational (RST) invariant features (7 numbers), and eccentricity extracted are extracted angularly from MOD-LBP. Based on the error value obtained using individual features, each feature will be assigned a weight,  $w$  which is the reciprocal of its corresponding error. Thus the features which yield less error get more importance in the retrieval process and error gets reduced. In order to achieve

users level of satisfaction, the weights can again be modified by multiplying with  $w^i$ ,  $i = 1, 2, 3...$  Table III shows the mean retrieval error in retrieving relevant image using different methods. Here reweighting has been done only one time. The Results reveal that the spatial Moments & histogram performs better than that of non-spatial in retrieving relevant slices from both T1-weighted and T2 weighted images. It is also observed the histogram and moment features with smaller window size captures discriminant information from the images. As number of angular region increases the retrieval error is gets reduced. The reweighting the moment features in the first time itself reduces the error remarkably.

TABLE III  
MEAN RETRIEVAL ERROR OF RETRIEVING T2-WEIGHTED IMAGES FROM T1-WEIGHTED IMAGES AND VICE VERSA USING (A) HISTOGRAM OF MOD-LBP (B) MOMENT FEATURES OF MOD-LBP (C) RELEVANT FEED MECHANISM BY REWEIGHTING THE MOMENT FEATURES

		Spatial					
		Non-Spatial	Angular Regions				
			2	4	6	9	18
T1 weighted images similar to T2 images	(a)	31.3	36.7	27.6	23.7	19.9	20.7
	(b)	55.8	20.5	15.0	17.3	13.7	10.4
	(c)		8.15	5.88	3.75	1.7	2.36
T2 weighted images similar to	(a)	26.5	19.7	14.1	10.5	10.4	10.1
	(b)	42.0	28.4	20.0	25.7	22.4	20.1
T1-weighted images	(c)		18.7	8.59	11.9	13.4	11.5

#### IV. CONCLUSION

The paper illustrates a method to retrieve T2 weighted axial images from T1 weighted images and vice versa. The result reveals the robustness of local measure to intensity related

problems. It also shows that the spatial moments of MOD-LBP acts a good descriptor for retrieving similar MR slices. It is observed that performance of the retrieval can be brought to users' level of satisfaction by reweighting the moment features. The method is applied to retrieve images from a single subject data as well as data across the subjects which would help the expert in the decision-diagnosis process. As the method is rotational and translational invariant, the costlier registration can be avoided and it is very easy to compute. The method can be extended to retrieve coronal and sagittal slices.

#### APPENDIX- A

Hu [14] proposed Moment Invariants (MI) for two-dimensional pattern recognition applications. For a digital image  $f(x, y)$ , the two-dimensional moment of order  $(p + q)$  is defined as:

$$m_{pq} = \sum_p \sum_q x^p y^q f(x, y) \quad (\text{A-1})$$

where  $p, q = 0, 1, 2, \dots$ . Translation invariance can be achieved by using central moment defined as follows.

$$\mu_{pq} = \sum_p \sum_q (x - \bar{x})^p (y - \bar{y})^q f(x, y) \quad (\text{A-2})$$

where  $\bar{x} = \frac{m_{10}}{m_{00}}, \bar{y} = \frac{m_{01}}{m_{00}}$ . The scaling invariant may be

obtained by further normalizing  $\mu_{pq}$  as:

$$\eta_{pq} = \frac{\mu_{pq}}{\mu_{00}^{\frac{p+q}{2}+1}} \quad (\text{A-3})$$

Using this, a set of seven Rotational scaling & translational invariant features (RST) are derived by Schalkoff [15]. The relative difference in magnitude of the Eigen values are thus an indication of the eccentricity of the image, or how elongated it is. The eccentricity is:

$$\sqrt{1 - \frac{\lambda_2}{\lambda_1}} \quad (\text{A-4})$$

where  $\lambda_1, \lambda_2$  are the Eigen value of the co-variance matrix

$$\begin{pmatrix} \mu'_{20} & \mu'_{11} \\ \mu'_{11} & \mu'_{02} \end{pmatrix},$$

where  $\mu'_{20} = \frac{\mu_{20}}{\mu_{00}}, \mu'_{02} = \frac{\mu_{02}}{\mu_{00}}, \mu'_{11} = \frac{\mu_{11}}{\mu_{00}}$ .

#### REFERENCES

- [1] G. Bucci, S. Cagnoni, and R. D. Domenicis, "Integrating content-based retrieval in a medical image reference database", *Comput. Med. Imag. Graph.*, vol. 20, no. 4, pp. 231-241, 1996
- [2] A. Qudus and O. Basir, "Wavelet based MR 2D slice retrieval in 3D volumes," in *Proc. IEEE Toronto Int. Conf.-Sci. Technol. Humanity*, Sep., 2009, pp. 545-550.
- [3] Azhar Qudus, and Otman Basir, "Semantic Image Retrieval in Magnetic Resonance Brain Volumes", *IEEE transactions on information technology in biomedicine*, Vol. 16, NO. 3, May 2012.
- [4] D. Unay, A. Ekin, and R. Jasinschi, "Medical image search and retrieval using local binary patterns and KLT feature points," in *Proc. Int. Conf. Image Process.*, 2008, pp. 997-1000
- [5] D. Unay, A. Ekin, and R. Jasinschi. "Local Structure-Based Region-Of-Interest Retrieval in brain MR Images," *IEEE Transactions on Information technology in Biomedicine*, vol.14, No.4, July 2010.
- [6] A. Rao and R. K. Srihari, Z. Zhang, "Spatial color histograms for content based image retrieval," in *Proc. IEEE Int. Conf. Tools Artif. Intell.*, Chicago, USA, 1999, pp. 183-186.
- [7] Ojala T, Pietikainen M, Maenpaa T. "Multiresolution gray-scale and rotation invariant texture classification with local binary patterns", *IEEE Trans Pattern Anal Mach Intell*, 24(7):971-87, 2002.
- [8] D. Unay, A. Ekin, and R. Jasinschi, "Medical image search and retrieval using local binary patterns and KLT feature points," in *Proc. Int. Conf. Image Process.*, 2008, pp. 997-1000
- [9] A. Varghese, B. Kannan, R. R Varghese, J.S Paul, "Level Identification in Brain MR images using Histogram of a LBP variant", *IEEE International Conference on Computational Intelligence and Computing research*, 2012, pp.207-210
- [10] Zhang, J., Ye, L., "An Unified Framework Based on p-Norm for Feature aggregation in Content-Based Image Retrieval," *Ninth IEEE International Symposium on Multimedia*, pp. 195-201, (2007).
- [11] Deselaers, T., Weyand, T., Ney, H., "Image Retrieval and Annotation Using Maximum Entropy," *CLEF Workshop 2006*, Alicante, Spain, (2006).
- [12] <http://www.bic.mni.mcgill.ca/brainweb/>
- [13] Henning Muller, Wolfgang Muller, "Automated Benchmarking in Content Based Image Retrieval", work supported by *Swiss National Foundation for Scientific Research* (grant no. 2000-052426.97).
- [14] M K. Hu, "Visual Pattern Recognition by Moment invariants," *IRE Trans. Info. Theory*, vol. IT-8, pp.179-187, 1962
- [15] Schalkoff, Robert, "Digital Image Processing and Computer vision," 1989.